IMPROVING PHASE FIELD MODELS OF RECRYSTALLIZATION OF GERMANIUM ANTIMONY TELLURIDE THIN FILMS FOR TRANSMISSION MODELING

Benjamin Belfore and Sylvain Marsillac
Virginia Institute of Photovoltaics, Old Dominion University, Norfolk Virginia

Abstract

Infrared Spectral Imaging is a fundamental imaging technique used in atmospheric and astronomy imaging fields. While filter wheels are one of the primary pieces of equipment used in infrared imaging, these filter wheels can have a significant Size Weight and Power (SWaP) burden. One way to decrease this burden is to change from these traditional filter wheel assemblies to filters based on phase changing materials. One of the more appealing technologies for implementation are Midwave infrared (MWIR) range are filters based on phase changing material like Germanium Antimony Telluride (GST). GST exploits the difference in refractive index between its various phases to act as a band pass filter. While these filters have been successfully created, over multiple heating cycles inhomogeneities could potentially form in the film and cause various problems. The following proceedings compound on optical and recrystallization simulations previously reported with the primary goal of refining the quality of the phase field simulations.

Introduction

MWIR band is a spectral region that spans wavelengths from 3 to 5 μm. This region is key to many analytical techniques. In the infrared region, most materials are near transparent. However, at very specific wavelengths, there is a resonant frequency where the chemical bonds absorb a given wavelength of vibration. This results in a significant increase in absorption at that given wavelength. By examining which wavelengths of light are preferentially absorbed, information about the presence of different chemical species and their relative abundance can be inferred. The MWIR band is also a region of which thermal imaging is of concern. In the MWIR region temperature based spectral imaging can be performed on various celestial bodies to obtain valuable information, For, NASA, the MWIR band is important for both atmospheric and space applications. For atmospheric sciences, the MWIR region can determine information about the amount and localization of gases. Some of the gases that resonate in the MWIR are methane (CH_4), Water, and CO_2. Being able to detect these and a variety of other gases are key to track key metrics of climate change. For space applications, using MWIR imaging is an important method for determining things like temperature irregularities of celestial bodies.

Conventional technology for MWIR filters for satellites use technologies based on filter wheels. In a filter wheel, filters of various wavelengths are spun at a given speed to detect different IR spectral emissions. Unfortunately, these filters can have an undo SWaP burdens. Since filter wheels contain multiple moving parts, ensuring continuous actuation over the entire lifetime of a satellite is also an area of concern [1,2,3,4].

One way to address both of these concerns simultaneously is to switch from a conventional filter wheel technology to one based on phase changing materials. One potential candidate for phase change infrared filters is Germanium Antimony Telluride (GST). GST is unique because depending on its crystalline phase: Amorphous, Face-Centered Cubic (FCC), and Hexagonal Closed Packed (HCP) both its optical and electronic properties can change significantly. Because of this

behavior, GST has been used in many technologies including rewritable CDs and Phase Change Memory. Because of the significant difference in refractive index between the various phases of GST in the MWIR range, GST is an excellent candidate for implementation in MWIR imaging filters.

Previously, work was done modeling how inhomogeneities in GST could potential be detrimental to the optical properties of GST films [6,7]. While successful, the definition and simulation of the recrystallization in these films was lacking. One such way that the initial simulations was lacking was the definition of the initial domain of the simulation. These simulations were done using a Voronoi diagram as the initial domain, and, while these domains were randomly assigned, the structure of the Voronoi diagrams proved to be detrimental to multiple facets of the simulation. For one, while the initial tessellations were randomly assigned a crystal orientation, the variance in size of the tessellations could have a significant impact on the final domain structure. Also, since the Voronoi diagram acted as the initial geometry, this initial condition was the state that the meshing would be defined as. Because the geometry within the system is inherently dynamic, an area that may need a high degree of definition initially may not near the end. To achieve sufficiently accurate results a very fine mesh would then be needed to account for how the domain changed through the simulation. These high density meshes resulted in significantly longer simulation times and were not well optimized to the simulation results. By being able to dynamically change the density of the mesh during the simulation, it is possible to utilize a coarser mesh in regions of lower interest while still having a high density where properties are changing.

Simulation Methodology, Refinement, and Results

To model these new meshing and recrystallization, phase field simulations were done using COMSOL Multiphysics as the PDE solver. Only the custom math module was used. The methodology for modeling phase field and the equations used are summarized below.

Phase Field

While multiple simulation techniques can be used to model recrystallization, phase field is appealing because it is an equation-driven non-statistical method. That means that, as additional information about a material system is obtained, various phenomenological and energy fields can be used to model the recrystallization process. One of the key limitations of phase field simulations, the indirect relationship between simulation time and real time, can also be mitigated when the general time scale of the recrystallization process is known. For GST, the time for crystallization and amorphization times is on the scale of ns, so in further simulation processes these time scales can be considered and contextualized.

In phase field simulations, the values of field variables η are solved for. η_i is a continuous, non-conserved field variable whose value varies between 1 within its domain and 0 outside of its domain. Phase field simulations can have an infinite number of phases, but, for higher end simulations, anything greater than 36 phases has no material impact on the results of the simulations [8]. Different field variables can be thought of as different grain structures or orientations with user defined variables specifying the energy or relaxation around different discrete field variables. There are two key equations that drive phase field simulations. The first of which is the time-dependent Ginsburg Landau Equation.

$$\frac{\partial \eta_i(r,t)}{\partial t} = -L_i \frac{\delta F}{\delta \eta_i(r,t)} \; i = 1,2,\dots,n \tag{1}$$

Where η_i is the field variable, L_i is the relaxation coefficient and r is related to the spatial dimension. F defines the grain boundary energy within the system. For our purposes F can be defined as:

$$F = \int_V f(\eta_1,\dots,\eta_n) + \sum_{i=1}^{n} \frac{\kappa_i}{2} (\nabla \eta_i)^2 \, dV \tag{2}$$

Where κ is the gradient of free energy density and f is local free energy density which we define as:

$$f(\eta_1,\dots,\eta_n) = \sum_{i=1}^{n} (-\frac{\alpha}{2}(\eta_i)^2 + \frac{\beta}{4}(\eta_i)^4 + \gamma \sum_{i=1}^{n} \sum_{j \neq i}^{n} \eta_i^2 \eta_j^2 \tag{3}$$

Where α, β, and γ are phenomenological constant. For our simulations, they are assumed to be 1. While potentially infinite numbers of η can be defined, due to the nonlinear nature of F, both the time and resources required to solve simulations of increasing numbers for field variables is highly nonlinear [8,9].

Within the math module in COMSOL the coefficient form PDE within the math module was used. The equation has the following general form:

$$e_a \frac{\partial^2 u}{\partial t^2} + d_a \frac{\partial u}{\partial t} + \nabla \cdot (-c\nabla u - \alpha u + \gamma) + \beta \cdot \nabla u + a u = f \tag{4}$$

The only variables in the equation above that are nonzero for our smulations are c, d_a and a. After inputting the correct variables for c, d_a, and a the final equation that is being solved for can be summarized for η_1 for a 4 field phase field simulation can be summarized as:

$$\frac{\partial \eta_1}{\partial t} = -\nabla \cdot (-2\nabla \eta) - \eta_1(-1 + \eta_1^2 + 2(\eta_2^2 + \eta_3^2 + \eta_4^2)) \tag{5}$$

As equation 5 shows, the complexity of the systems increases significantly with the number of phases, to address this, for these preliminary tests, a four-phase system was used. This ensured that rapid testing of various phenomena could be done quickly and efficiently.

Previous Geometry

Now that the equations have been established, the domain of the simulation needs to be addressed. In previous simulations, Voronoi diagrams were used as the initial condition. An example of a Voronoi diagram, its initial meshing, and the simulation results at t_{final} are shown below.

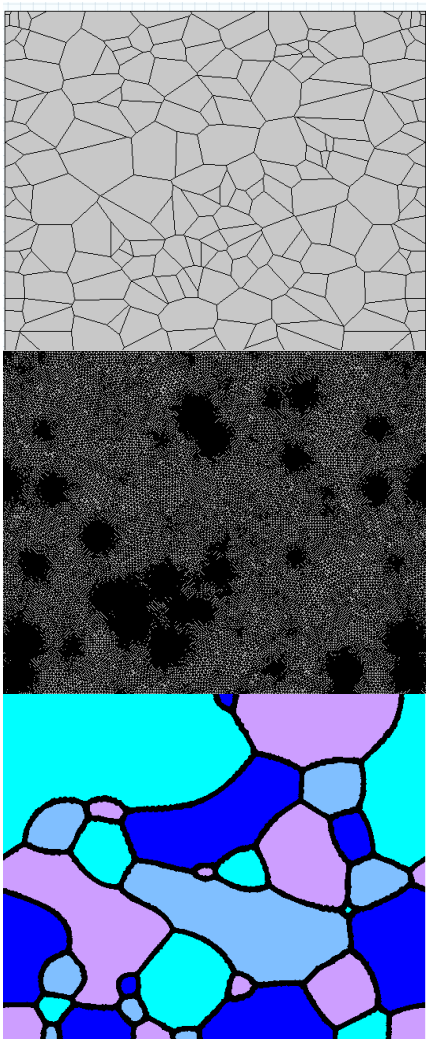

Figure 1: Initial Voronoi Diagram (top) Model Meshing (middle) and final simulation results (bottom).

As figure 1 shows, the initial meshing is extremely dense through the entire domain which the mesh becoming even more dense in regions where multiple tessellations meet. When examining the final result however, the areas that needed initially a high degree of mesh density don't necessarily need it anymore. To compensate for this a high mesh density has to be used everywhere to ensure an accurate final simulation. Such a method has a significantly negative impact on simulation times.

New Geometry

Transitioning from a Voronoi tessellation domain to a uniform domain with random phase assignments has several distinct advantages. First, since the mesh is defined by initial geometry of the domain, a defined mesh density will result in a more evenly disturbed mesh. A more uniform mesh will behave better as the domain evolves over simulated time. The other key advantage of using such a geometry is the ease at which the mesh can further be refined during the simulations. The primary area of interest is where one field variable changes to another. Outside of this region nothing is happening form a computational perspective, so the mesh can be coarser. Utilizing a uniform mesh can mitigate potential areas of localized high error within the simulation. Since the mesh is coarser generally, doing adaptive mesh refinement during the simulation also becomes a viable alternative to a basic, high-density mesh

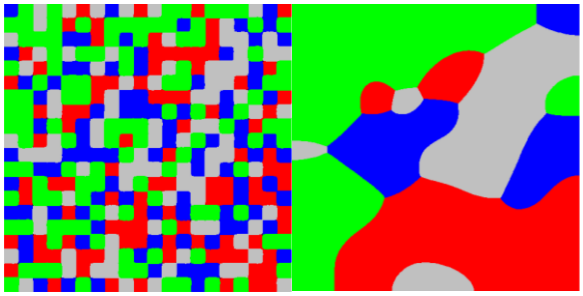

Figure 2: Initial condition of the initial randomized uniform domain (left) and the domain at T=800 (right).

As the figure above shows, the new geometry contains an array of basic square domains. These domains are then randomly assigned to one of the four phases using a normal distribution. Then using COMSOL Eq(4) is solved over the domain. At discrete time

intervals within the simulation, an adaptive mesh refinement was performed based on how the boundaries between the domains are defined. The grain boudnaries between domains in a phase field simulations is anywhere

$$(\eta_1^2 + \eta_2^2 + \eta_3^2 + \eta_4^2)^{\frac{1}{2}} < 1 \quad (6)$$

This is because within a field, one of the field variables will always equal 1 and the others 0, and, since the value of a field variable can never be greater than 1, on the interfaces, the magnitude of the field variables can never be grater than one. Equation 6 was the equation that governed how the mesh was refined.

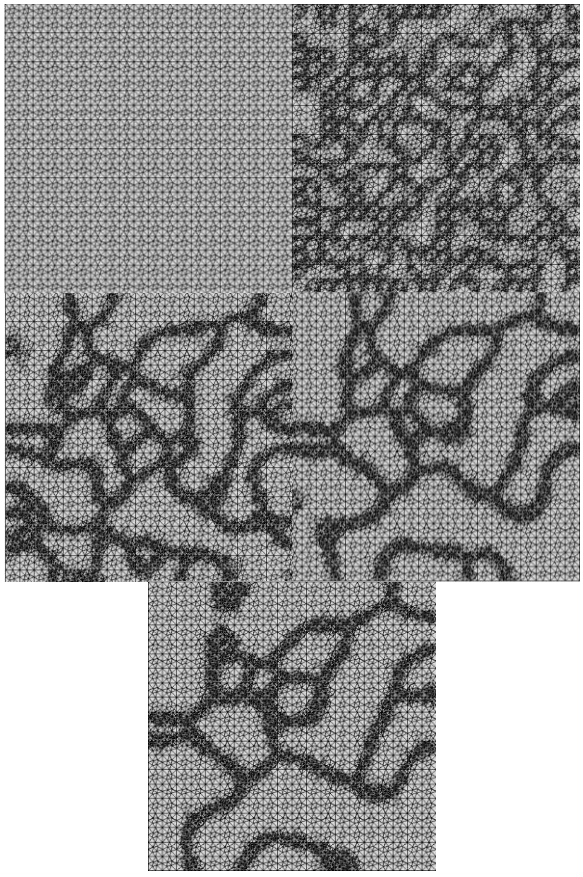

Figure 3: Adaptive mesh refinement from the initial uniform mesh (top left) to the final mesh (bottom)

Figure 3 shows how the mesh refines as the simulation time increases. Initially, the first mesh is a relatively coarse, uniform mesh. As domains begin to coalesce, the mesh maintains the same density within the field variables but becomes more fine at the interfaces. As the microstructure continues to evolve the mesh continues to coarsen back to its default state. While this methodology increases simulation time, the difference in the final microstructure is different to a meaningful extent.

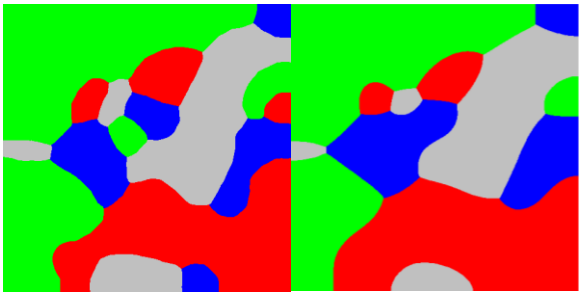

Figure 4 Simulation without adaptive mesh refinement (left) and with mesh refinement (right)

As figure 4 shows using an adaptive mesh refinement to improve mesh density at interfaces can change the results significantly. While this methodology increases simulation time, the difference in the final microstructure is different to a meaningful extent.

Conclusion

Non-uniform initial geometry resulted in a poor-quality mesh distribution, especially when the geometry of interest moved interfaces within the domain. Changing the geometry to more uniform initial conditions allowed for both more consistent and accurate simulation results. To further improve the quality of simulations, adaptive mesh refinement was implemented. These adaptive measurements tracked the new interfaces within the domain to improve the precision of the numerical simulations in these localized regions. The implementation of these two modifications resulted in higher quality recrystallization simulations, which can now be used for future optical simulations of phase change materials.

Acknowledgements

This research was funded via a graduate research fellowship through the Virginia Space Grant Consortium. I would also like to acknowledge Dr. Orlando Ayala of Old Dominion University for providing additional guidance and teaching me the fundamentals of COMSOL Multiphysics.

References

[1] G. J. Hawkins, R. E. Sherwood, B. M. Barrett, M. Wallace, H. J. B. Orr, K. Matthews, and S. Bisht, "High-performance infrared narrow-bandpass filters for the Indian National Satellite System meteorological instrument (INSAT-3D)," Appl. Opt. 47, 2346-2356 (2008).

[2] G. Shaw and H. Burke, "Spectral imaging for remote sensing", *Lincoln Lab. J.*, vol. 14, no. 1, pp. 3-28, 2003.

[3] Calum Williams, Nina Hong, Matthew Julian, Stephen Borg, and Hyun Jung Kim, "Tunable mid-wave infrared Fabry-Perot bandpass filters using phase-change GeSbTe," Opt. Express 28, 10583-10594 (2020).

[4] A. Rogolaski. "Infrered detectors: an overview," *Infrared Physics and Technology*, vol. 43, no. 3-5, pp. 187-210, 2002.

[5] H. -S. P. Wong *et al.*, "Phase Change Memory," in *Proceedings of the IEEE*, vol. 98, no. 12, pp. 2201-2227, Dec. 2010.

[6] Matthew N. Julian, Calum Williams, Stephen Borg, Scott Bartram, and Hyun Jung Kim, "Reversible optical tuning of GeSbTe phase-change metasurface spectral filters for mid-wave infrared imaging," Optica 7, 746-754 (2020).

[7] P. Guo, A. M. Sarangan, and I. Agha, "A review of germanium-antimony-telluride phase change materials for non-volatile memories and optical modulation," *Applied Sciences*, vol. 9, no. 3, pp. 530, February 2019.

[8]M.A. Zaeem, H.E. Kadiri, P. Wang, M. Ho rstemeyer "Investigating the effects of grain boundary energy anisotropy and second-phase particles on grain growth using a phase-field model" Comput. Mater. Sci. 50 ,pp. 2488-2492, (2011).

[9] N. Moelans, B. Blanpain, and P. Wollants,, "Phase field simulations of grain growth in two-dimensional systems containing finely dispersed second-phase particles" Acta Materialia, Volume 54, Issue 4,, pp. 1175-1184, 2006.